Energy content and ionization level in an argon gas jet heated by a high intensity arc

By GORDON L. CANN* and ADRIANO C. DUCATI
Giannini Research Laboratory, Santa Ana, California

(*Received* 20 *February* 1958)

SUMMARY

A direct current electric arc has been developed as a heating device for argon gas. Negligible amounts of electrode material are consumed during an operating time of several minutes. Under normal operating conditions 50% to 90% of the input electric power is transferred directly to the gas. The remaining power is absorbed by the water-cooled electrodes. Measurements were made to determine the total gas enthalpy and the proportion of the enthalpy in directed kinetic energy, random particle motion, and ionization energy. From these measurements it is postulated that the gas is initially in a non-equilibrium state on leaving the arc, but approaches equilibrium relatively quickly when confined to a constant diameter jet outside the arc. The gas temperature range in these experiments varies from 5000° K to 15000° K.

INTRODUCTION

The study of propulsion systems having a very high specific impulse and the investigation of various aerodynamic and aerothermal effects occurring at Mach numbers greater than 10 require gas flows with stagnation temperatures of several thousand degrees. An electric arc has proved to be a very effective means of heating a gas to such temperatures in a continuously operating device. Much work has been done in Germany in recent years on the water-stabilized arc utilizing carbon electrodes. The back electrode was usually a rod cooled by the water vortex. The front electrode was a carbon plate with an orifice directly in front of the rod through which a jet of water and carbon vapour escaped when the arc was in operation. The development at the Giannini Research Laboratory of a continuously operating arc to heat a jet of inert gas has made it possible to study the state of the gas immediately upon leaving the arc and at subsequent times by confining the gas flow to a water-cooled channel. From the gas dynamics of the flow and experimental measurements of thrust, mass flow rate, and the total energy balances, it is possible to deduce the amount of energy in the gas in the form of directed kinetic energy, random particle motion, and ionization. In the results reported here, argon was used exclusively.

* Now at the California Institute of Technology, Pasadena, California.

Experimental equipment

Figure 1 is a schematic diagram of the electric arc used to heat the gas. The electrodes consist of two metal plates, one with an orifice through which the gas escapes. The plates are water-cooled and enclosed by a water-cooled cylinder through which the gas is fed tangentially into the arc chamber. The arc strikes between the edge of the orifice and the back plate. Gas near the outer edge of the hole receives significantly less energy than that which passes through the centre of the arc. The energy exchange process appears to be unaffected by either reversal of the polarity of the electrode or radial, rather than tangential, introduction of the gas.

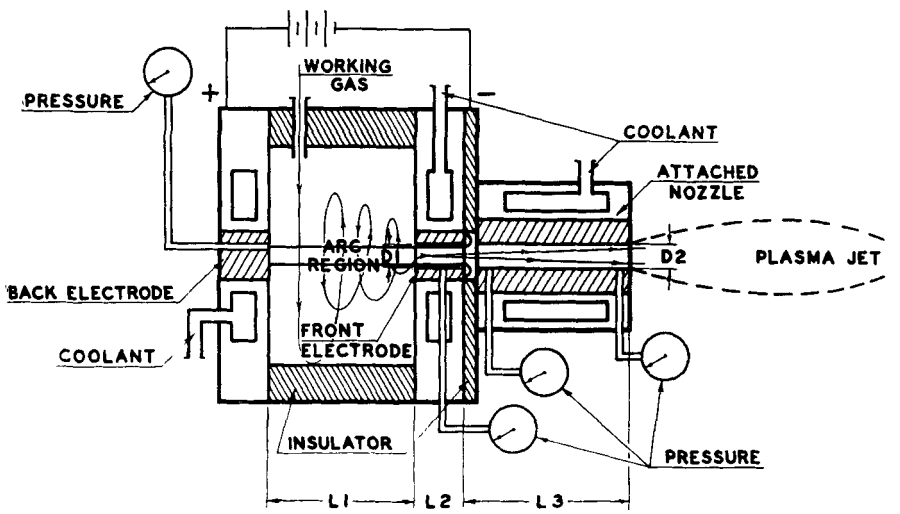

Figure 1. Schematic drawing of typical device used for arcing through the gas. A nozzle is shown in position, electrically insulated from the front electrode of the arc.

Figure 2 (plate 1) shows the general arrangement of the equipment and essential instrumentation. The thrust developed by the gas jet was measured by observing the deflection of a cantilever mounting bar. Flowmeters measured the rate of flow of the gas and cooling water. The power lost in the electrodes could be determined by noting the temperature change of the cooling water. The electrical power input was measured during each run and a bank of gauges registered the pressure at various points in the arc and confined jet.

Jet characteristics

Once the gas has left the arc chamber and entered the cylindrical channel, diffusion processes tend to equalize enthalpy and velocity in the radial direction. Since the Reynolds number is quite large and the nozzle length was never more than five times the diameter, boundary-layer effects

were ignored in the calculations. Ambipolar diffusion, thermal diffusion, and diffusion by concentration gradients are all occurring simultaneously; hence no effort was made to calculate the radial distribution functions. However, an estimate of the effect of radial distributions of velocity and temperature was made in the following manner. First, Gaussian distribution functions were assumed for velocity and temperature. Then the average values of these quantities were determined for various distribution parameters and these average values compared with the results calculated assuming no radial variation. The enthalpy and velocity proved to be least sensitive to the radial distribution parameter. With a radial temperature ratio of 20 (approximately room temperature at the outside) and a velocity ratio variation of 4·5, the result of averaging over a Gaussian curve would be to increase the velocity and enthalpy by about 20% over the values obtained by assuming no radial variations. The average temperature under these conditions would be 70% higher than the temperature for no radial variations.

A rough estimate of the fraction of the gas affected by the boundary layer can be made by measuring the power carried away by the cooling water of the nozzle. If r_1 is the effective radius of the edge of the boundary layer, a the radius of the channel, and P_w the power absorbed in the nozzle cooling water, then

$$P_w = 2\pi \int_{r_1}^{a} (h_0 - h)\rho u r \, dr, \tag{1}$$

where $(h_0 - h)$ is the enthalpy decrement across the nozzle. From this relation, the mass flow in the boundary layer can be found. This calculation assumes a uniform initial distribution of enthalpy throughout the gas, which is certainly incorrect, and the answer can be taken as only a rough indication of the fraction of the mass flow affected by the boundary layer. With these restrictions, the calculations indicate that sometimes as much as 60% of the mass flow can be within the boundary layer. However, the actual physical extent of the boundary layer is a small fraction of the channel diameter, due to the much higher gas density in the vicinity of the walls. The region of cooled gas can be seen very clearly in figure 3 (plate 1).

In order to analyse the gas flow, the following assumptions have been made:

(*a*) electrical energy is transferred to the gas in a channel of the same diameter as the hole in the front electrode and mass is added continuously along the length of the arc;

(*b*) radial variation of temperature, density and velocity are neglected;

(*c*) the energy in electronic excitation is negligible (for the temperature and densities used here, Resler, Lin & Kantrowitz (1952) have shown that this introduces no appreciable error);

(*d*) the axial pressure gradient due to the magnetic field of the arc is neglected (the magnetic pressure was calculated to be less than 3% of the static gas pressure for the current densities and gas pressures used).

The equation of state for a noble gas in which the temperature is high enough to produce ionization may be written

$$p = \rho R(T_G + \alpha T_e); \tag{2}$$

and the enthalpy of the gas is given by

$$h = \frac{\gamma_0}{\gamma_0 - 1}\frac{p}{\rho} + \alpha j. \tag{3}$$

Definition of the symbols is provided at the end of the paper. The equilibrium degree of ionization, α, is given as a function of the temperature T by the Saha equation:

$$\frac{\alpha^2}{1-\alpha^2}\frac{p}{p_a} = \frac{\Delta E_0^0}{RT} - \frac{\Delta(F^0 - E_0^0)}{RT}. \tag{4}$$

Values for the free energies (ΔF^0) were obtained from a report by Gilmore (1955). By combining these equations with the gas-dynamic equations, it is possible to relate the exit gas velocity μ_E, temperature T_E, and degree of ionization α_E to the various measured parameters such as thrust F, channel exit pressure p_E, mass flow rate $\dot{m}$, and power input to the gas P_G.

When

$$F \geqslant \gamma_0 A p_a,$$

the flow in the orifice is critical and this criterion was used in the experiments to determine whether the flow at the nozzle was sonic or subsonic.

For the critical flow the following set of equations was derived from one-dimensional flow theory (Cann & Ducati 1957). The velocity is related to the thrust and mass flow rate by

$$\mu_E = \frac{\gamma_0}{\gamma_0 - 1}\frac{F + Ap_a}{\dot{m}}. \tag{5}$$

The degree of ionization is obtained from the equation

$$\left(\frac{P_G}{\dot{m}} - \alpha j\right)_E = \frac{\gamma_0^2}{2(\gamma_0^2 - 1)}\left(\frac{F + Ap_a}{\dot{m}}\right)^2, \tag{6}$$

and the temperature is given by

$$(T_G + \alpha T_e)_E = \frac{\gamma_0}{(\gamma_0 + 1)^2 R}\left(\frac{F + Ap_a}{\dot{m}}\right)^2. \tag{7}$$

In some cases, the exit pressure was checked by using the result

$$Ap_E = \frac{F + Ap_a}{\gamma_0 + 1} = \frac{Ap_0}{\gamma_0 + 1}. \tag{8}$$

For subcritical flow in the orifice, the above equations are changed to the following set. The velocity is now given by

$$\mu_E = F/\dot{m}. \tag{5 a}$$

The degree of ionization becomes

$$\left(\frac{P_G}{\dot{m}} - \alpha j\right)_E = \frac{\gamma_0}{\gamma_0 - 1}\frac{FAp_a}{\dot{m}}\left(1 + \frac{\gamma_0 - 1}{2\gamma_0}\frac{F}{Ap_a}\right), \tag{6 a}$$

and the temperature is now obtained from

$$(T_G + \alpha T_e)_E = \frac{FAp_a}{\dot{m}^2 R}, \tag{7 a}$$

with the pressure relation given simply by

$$p_E = p_a. \tag{8 a}$$

Discussion of results

(1) Table 1 shows some representative measurements. During the experiments the electric input power ranged from 10 kW to 100 kW; however, the power in the runs shown in table 1 ranged only between 30 kW and 50 kW. The thrust that the jet developed varied between one and ten newtons.

(1) $\dot{m}$ kgm/sec $\times 10^3$	(2) h kW-sec/kgm	(3) l in.	(4) α_E	(5) u_E m/sec	(6) $(u_E)_{eq}$ m/sec	(7) S.I. sec
2·98	6500	$\frac{1}{8}$	0·14	580	1800	58
5·07	5130	$\frac{1}{8}$	0·12	470	1600	47
9·06	3390	$\frac{1}{8}$	0·08	370	1300	40
5·04	3100	$\frac{1}{4}+1{\cdot}0$*	0	1250	1240	164
4·66	4030	$\frac{1}{4}+1{\cdot}0$*	0	1450	1420	195

Table 1. Results from a series of tests using argon in the plasma jet. The mass-flow rate, specific enthalpy, and front electrode length are measured directly. The exit flow velocity u_E and degree of ionization α_E are determined from equations (5) or (5 a), and (6) or (6 a), respectively; while the specific impulse is obtained from the definition S.I. $= F/\dot{m}g$; $(u_E)_{eq}$ is the predicted value of exit velocity assuming equilibrium in the gas at the exit. A one-inch nozzle was added in the two runs marked * in column (3).

(2) Using the configuration shown in figure 1, without a nozzle, the exit velocity obtained from the measured values of thrust and mass flow was always much lower than would be expected from a calculation using equilibrium thermodynamics. As can be noted from the first three lines in table 1, these values differ by a factor of two or three. The ionization level of the gas calculated from equation (6) or (6 a) was likewise much higher than the value predicted for equilibrium ionization, which should be negligible for the enthalpy given in column (2).

(3) The geometrical parameters of electrode spacing, orifice diameter, and thickness of the front electrode were varied over a considerable range. Although some improvement in performance was noted when the width of the front electrode was increased, in general the velocity and specific impulse remained considerably below the equilibrium values as described above. The average calculated ionization level remained much higher than the expected equilibrium level.

(4) The effect of varying the electrical parameters of the arc was also studied. The polarity was changed with no marked effect on the gas-dynamic performance, despite the fact that the point on the front electrode at which the arc struck moved from the outside to the inside when the polarity of the front electrode was changed from negative to positive. A wide range of average current densities was used with only a second-order effect on the exit gas-dynamic properties. There was an indication that at higher current densities the deviation from the average equilibrium exit conditions was more pronounced.

(5) The gas enthalpy and pressure were changed over the ranges 1000 kW sec/kgm to 12 000 kW sec/kgm and 18 psi to 150 psi, respectively. There was no measurable indication that either of these variables affected the noted discrepancy between the calculated and the equilibrium values of velocity and ionization level at the exit.

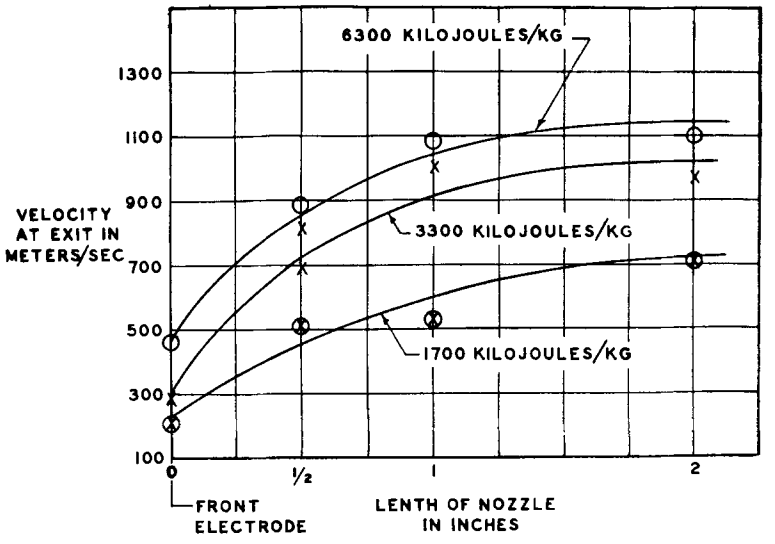

Figure 4. Exit velocity as a function of nozzle length for a 3/16-in. diameter nozzle. The gas used was argon.

(6) A series of nozzles was placed over the jet immediately downstream from the front electrode, from which they were electrically insulated. The nozzles were for the most part cylindrical and of the same diameter as the front electrode orifice. The length of the nozzles was varied from zero up to 10 nozzle diameters. There was a gradual trend toward equilibrium at the exit as the length of the nozzle was increased, and, for the longest nozzles, under some operating conditions, the measured exit gas velocity and ionization level agreed to within experimental error with the calculated equilibrium values. Figure 4 shows the effect of nozzle length on the exit velocity of the jet for three different enthalpy levels.

It can be seen that the exit velocity reaches approximately a constant value for nozzles longer than five nozzle diameters.

(7) Examination of the back electrode indicated that the arc struck over an area equal to that of the orifice in the front electrode; however, no estimate could be made of the radial distribution of current density. When the back electrode was the anode, the power in watts measured in the anode cooling water was numerically about 10 to 15 times the current in amperes through the arc. This indicates an anode potential drop of 10 to 15 volts, which represents the voltage through which the electrons are accelerated without suffering collisions with other electrons or gas atoms before impinging upon the anode surface. This value agrees quite well with values reported by Cobine & Burger (1955) for conventional arcs.

(8) Attempts to correlate the power absorbed by the front electrode and nozzle were never very successful. The best approach appeared to be aerodynamic heat-transfer calculations. By using the simple heat-transfer equation for turbulent boundary layers, the power absorbed by the cooling water of the front electrode could be calculated to within a factor of two.

(9) The power radiated from the front orifice and the jet was measured to determine if any appreciable fraction of the input electrical power was lost from the gas in the form of electromagnetic radiation. The spectrograms indicated a fairly intense continuum radiation, as well as numerous lines. From calorimetric measurements of the total radiant flux, it was found that at most 5% of the input power was radiated. This effect was not included in the calculations, as it was of the order of the experimental errors of measurement.

The following model has been postulated to explain the behaviour noted above. While the gas is passing through the arc, the electric power is transferred to a small core of gas at the centre of the orifice, indicated as region *ab* in figure 5; this region, encompassing only a small fraction of the total mass flow, does not appreciably increase in radius due to the pinching effect of the arc's own magnetic field. Once the gas leaves the arc, radial diffusion of enthalpy occurs and a larger percentage of the gas is heated up (region *bc*). Simultaneously, for the cases where a nozzle is added after the orifice, a cool boundary layer is formed along the outer radius that encompasses more and more of the mass flow as the channel length is increased. As long as the outward radial flow of enthalpy is faster than the radial inward growth of the boundary layer, the flow will behave as indicated in (6) above. An axial pressure drop along the nozzle was measured in the tests and appears to result from the volume heating effect of the radial diffusion of enthalpy and the transformation of ionization energy into random particle motion.

With the above model, equilibrium calculations were carried out to see if all experimentally determined quantities could be accounted for. When a nozzle was not used, the equilibrium ionization level found from the calculations was always low by a factor of two or more from the measured value. If the central core of gas in the arc region were in equilibrium,

there would be a fairly large radial enthalpy outflow due to the high temperature gradients. However, the measurements indicate that no appreciable radial enthalpy flow occurs in the presence of the electric field since lengthening the front electrode did not affect the thrust for a given power and mass-flow.

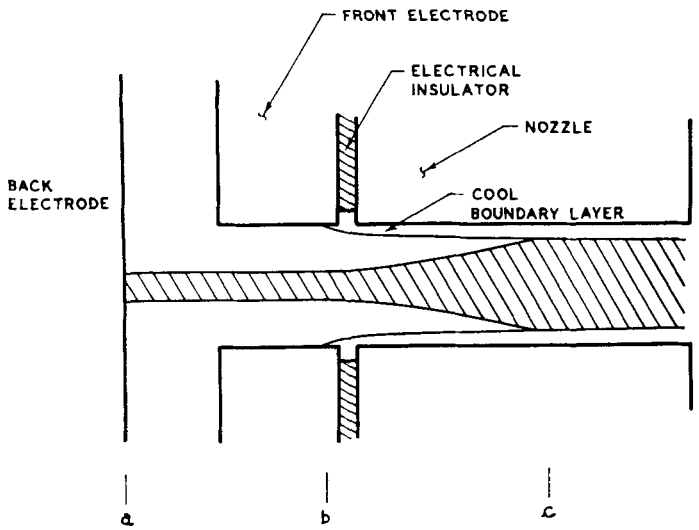

Figure 5. Diagram indicating the proposed energy exchange processes occurring in the jet. The enthalpy is transferred to the gas in the core of the arc between *a* and *b*. From *b* to *c* the enthalpy diffuses radially outward until it intersects the boundary layer region. From *c* on there is a hot central core surrounded by the expanding cool boundary layer.

Therefore, it is tentatively concluded that the gas is not in temperature equilibrium in the arc region and in the region immediately downstream from the arc; the electron temperature and ionization level in these regions must be considerably higher than the equilibrium values.

The authors would like to extend their thanks to Professor H. W. Liepmann of the California Institute of Technology for his many helpful suggestions during the course of this work. We would also like to acknowledge the invaluable assistance in preparing and proof-reading the report rendered by Dr V. H. Blackman of Giannini Research Laboratory.

This research was supported by the United States Air Force through the Air Force Office of Scientific Research of the Air Research and Development Command under Contract No. AF 49(638)–54.

LIST OF SYMBOLS

A	cross-sectional area of gas flow channel,	ΔE_0^0	ionization energy,
		F	thrust,
E_0^0	ground state internal energy level,	F^0	free energy,
		h	specific enthalpy,

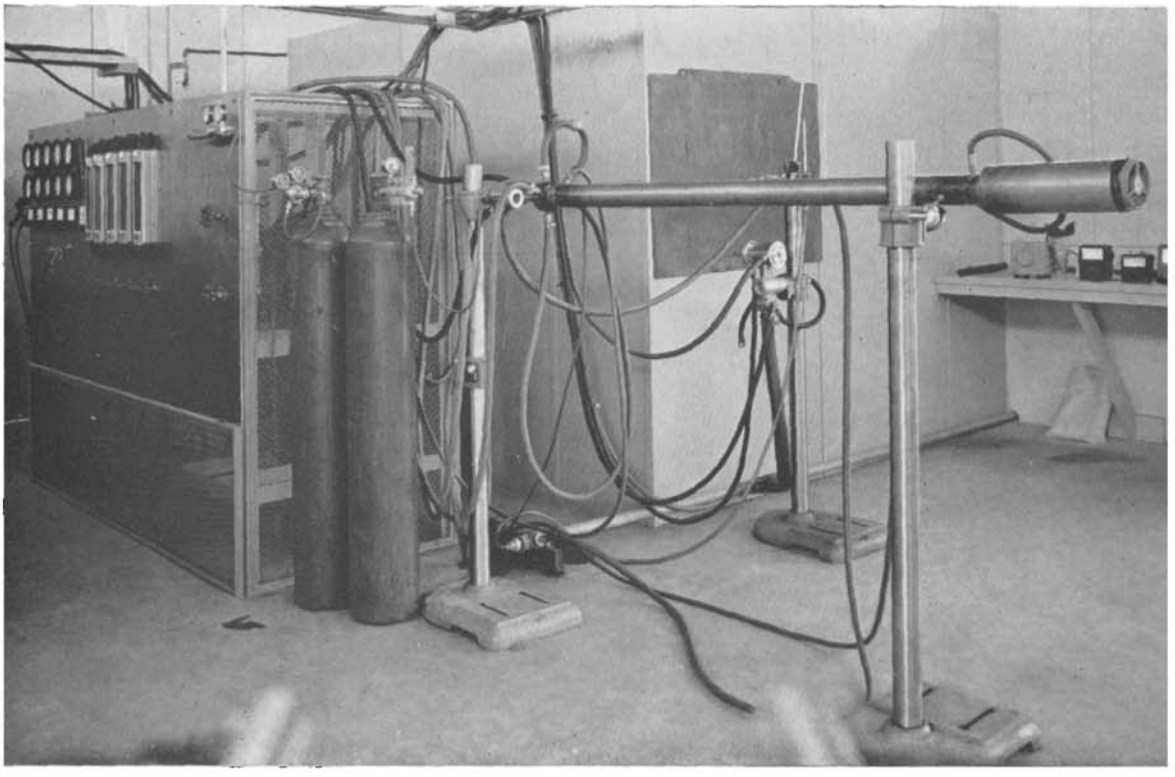

Figure 2. Instrument panel showing the equipment and essential instrumentation used during the majority of the tests.

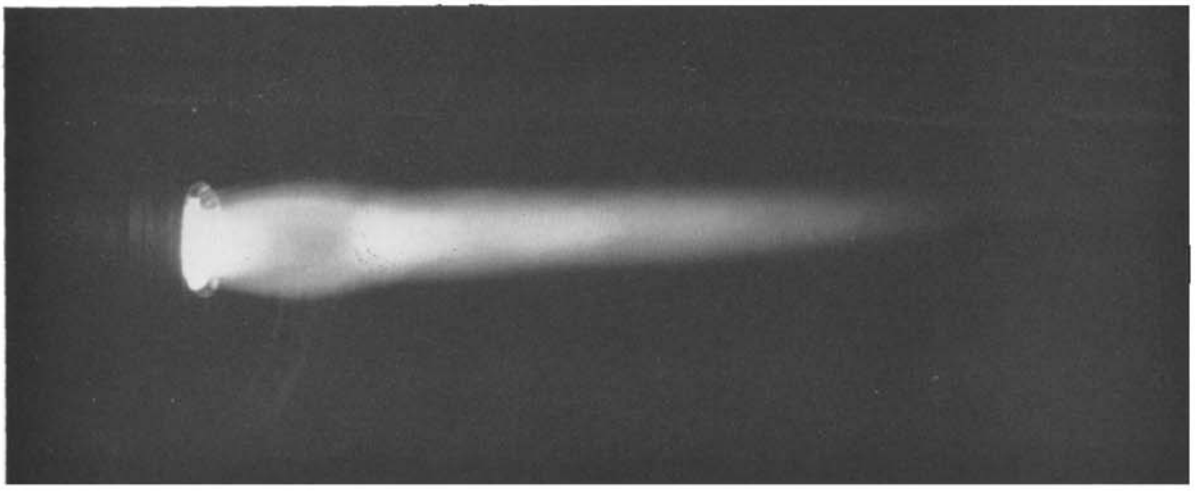

Figure 3. Photograph of the plasma jet exhaust showing the region of non-luminous flow near the nozzle walls. Standing shock waves can be seen clearly.

j	specific ionization energy,	R	gas constant,
l	front electrode length, e.g. $\frac{1}{8}+1{\cdot}0$ represents a $\frac{1}{8}$-in. thick front electrode with a 1·0-in. long cylindrical nozzle,	S.I.	specific impulse,
		T	temperature,
		T_e	electron temperature,
		T_G	gas temperature,
		u	gas velocity,
$\dot{m}$	gas mass flow rate,	α	fraction of gas ionized,
p	gas pressure,	ρ	gas density,
p_a	atmospheric pressure,	γ_0	1·67, not necessarily the ratio of the specific heats.
P_G	power in the gas,		

Subscript E refers to conditions at the channel exit.

References

Cann, G. L. & Ducati, A. C. 1957 Propulsive properties of high intensity plasma jets, *Giannini Research Laboratory, Report* no. TR–9.

Cobine, J. D. & Burger, E. E. 1955 *J. Appl. Phys.* **26,** 895.

Gilmore, R. F. 1955 Equilibrium composition and thermodynamic properties of air to 24 000° K, *Rand Corporation, Report* no. RM–1543.

Resler, E., Lin, S. & Kantrowitz, A. 1952 *J. Appl. Phys.* **23,** 1390.